Delay Alignment Control for 5G Multi Connectivity

Katrina Lau, Torbjörn Wigren, Richard H. Middleton and Ramón A. Delgado

***Abstract*— In fifth generation wireless systems, multi-point transmission will be used to counter the increasing radio shadowing at high carrier frequencies. Due to fading and varying delays over the IP-connections to the transmission nodes, the travel time of data from the source to the application may vary significantly between the different transmission paths. In case of e.g. video streaming this could result in packet re-ordering problems, leading to protocol resets. The paper therefore develops and evaluates a new delay alignment feedback controller that simultaneously aims to control the delay and the delay skew between the transmission paths. Simulations illustrate the performance of the proposed data flow delay controller. The delay skew controller is also analyzed and proved to yield a globally $\mathcal{L}_2$ stable feedback system.**

I. Introduction

The high capacity and low latency of new fifth generation (5G) air interfaces are intended to enable new mobile wireless solutions, e.g. by extension of today's wired augmented reality (AR) and virtual reality (VR) applications. AR may e.g. use streaming wireless video to overlay real time 3D models on top of visually observed objects, to support operators at industrial production lines [1], [2]. Wireless VR devices and applications are expected to make the tactile internet available wherever there is 5G connectivity [3], [4]. These AR and VR use cases are both dependent on very low end-to-end delay, with low jitter [5]. The present paper reflects this requirement and proposes a new delay alignment controller to mitigate end-to-end delay imperfections like those highlighted by Fig. 1. As can be seen, the delay impairments may be caused by the interplay between radio fading, transmission queue data dwell times, packet switched transport network delay variations, and the delay differences between the transmission paths of the multi-point transmission scheme. Multi-point transmission becomes increasingly important in 5G systems utilizing higher millimeter wave (mmW) carrier frequencies, because of significant radio shadowing experienced at these frequencies [6].

Previous work on delay control related to the present paper starts with the transmission control protocol (TCP) and the wide class of active queue management algorithms (AQM) [7], [8]. AQM algorithms discard packets prior to wireless transmission to provide early feedback to the transmitting TCP source, to achieve a reduced round trip delay. Since the AQM feedback is neither regular nor necessarily terminated in the data splitter node of Fig. 1, the achieved delay and jitter performance may not be sufficient for high end 5G applications. This can be improved by introducing inter-node synchronization and time stamping for measurement of the downlink and uplink network delays as in e.g. [9], [10] and the present paper. Another approach to the delay alignment problem would be to apply control methods that are robust to unknown delay and jitter, as e.g. in [11]. Buffering can also be used for mitigation of jitter, albeit at the cost of an associated back-off of the achievable end-to-end delay, see e.g. [12]. A multi-path architecture with delay control was treated in [13], where a statistical algorithm was used to optimize delay and delay skew for voice and video data.

The main contribution of the present paper is a delay alignment controller supporting 5G multi-point transmission. The controller uses the transmission node queues as actuators to achieve simultaneous end-to-end delay and delay skew control. One example application would be synchronization of video shown on a large public screen, but where viewers get high fidelity audio in their headsets to avoid disturbances from the surrounding environment.

The proposed controller differs from previous research by the authors in several ways. The first difference to previous research in, for example, [9] and [14] is that the outer loops of those papers are replaced by a static computation of reference values for the single path controllers handling each data path, using the measured momentary transport delays. This has some far-reaching impacts. First, the question of stability collapses to inner loop stability of each data path, since there is no outer loop feedback to consider. The inner loop stability is addressed by repeated use of the Popov criterion ([15]–[17]) in the present paper, using results of [18]. The Popov criterion is also used in [19], however that work is limited to a two node case, while the present paper treats n-node architectures. The works of [20] and [21] also treat n-node data path architectures, however these works need to use the more advanced Integral Quadratic Constraint (IQC) theory [22] for the stability analysis. The results in [23] are also based on [18], but those are applied to the control of end-to-end *round-trip* delays. As touched upon above, the second contribution of this paper is that it analyzes the input-output stability of the control system proposed in the paper. Here, the repeated use of the Popov-criterion results in conditions that guarantee the $\mathcal{L}_2$-stability of the multiple-input-multiple-output (MIMO) closed loop system. The third contribution is that simulations are used to test the performance. The numerical evaluation and comparison to the algorithm of [9] show that the proposed delay skew control algorithm performs better in that the delay and delay skews are regulated with smaller errors for the considered

Katrina Lau, Ramón A. Delgado and Richard H. Middleton are with the Priority Research Centre for Complex Dynamic Systems and Control, The University of Newcastle, Callaghan, NSW 2308, AUSTRALIA. e-mail: {k.lau, richard.middleton, ramon.delgado}@newcastle.edu.au.

Torbjörn Wigren is with L5GR Systems, Ericsson AB, Stockholm, SE-16480 Sweden. e-mail: torbjorn.wigren@ericsson.com.

Peer-reviewed author's copy of:
K. Lau, T. Wigren, R. H. Middleton and R. A. Delgado, **Delay Alignment Control for 5G Multi Connectivity**. In *2018 IEEE Conference on Decision and Control (CDC)*, Miami Beach, FL, 2018, pp. 7064-7070.
Available at https://doi.org/10.1109/CDC.2018.8619220

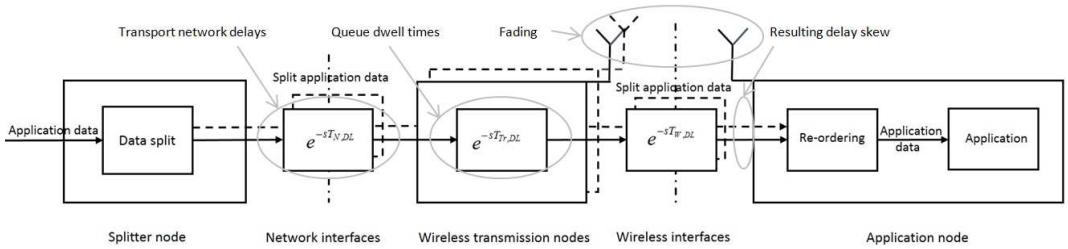

Fig. 1. High level block diagram of the end-to-end multi-path data flow and delay control system in the downlink delay skew control case. The main sources of radio and delay variations are encircled with gray color. Incoming application data is split and sent to multiple transmission nodes over multiple network interfaces, where each transmission node communicates with the application node over a separate air interface.

scenario. A discussion on the benefits and drawbacks of the proposed controller and the one of [9] is given as well.

The control system of the paper is defined in continuous time. For implementation, the algorithms are discretized with the Tustin approximation [24] as in [9], [14] and [18]. The notation exploits boldface characters to indicate vectors and matrices. The paper uses a mix of descriptions in time t, and in the Laplace transform domain s. When handling nonlinear transformations a swap to the time domain is required which is stated directly in the paper. Time domain signals are marked with an inverted caret as $\check{f}(t)$ where (t) indicates dependence of time.

The paper is organized as follows. The delay skew control system is described in Section II. The stability properties are analyzed in Section III. The performance of the control system is also evaluated numerically in Section IV. The paper ends with a discussion in Section V and conclusions in Section VI.

II. Delay aligning downlink feedback control

A block diagram of the MIMO delay skew controller is depicted in Fig. 2. This block diagram is valid for control of the delay skew defined from the data split node to the air-interface of each transmission path. This case is referred to as the downlink delay skew control case, and it is useful for time aligned data transmission at the air-interfaces to the application node. Tactile VR control applications in need of round-trip delay skew control should rather use the algorithms of [14] or [21].

The delay skew controller consists of an outer queue dwell time reference value compensation mechanism $\mathbf{M}$, described in Section II-A, and n inner control loops (one per transmission path) described in Section II-B. As can be seen in Fig. 2, the outer reference value compensation mechanism is described in the time domain, while the inner loops are mainly described in the Laplace transform domain to be consistent with prior work. The interfaces between the outer part and the inner loops are manifested by the multiplication and division operations that perform the embedding that enables time invariant inner loop controller design and time stability analysis, as described below.

The outer compensation mechanism computes $\Delta\check{T}_{skew,i}(t)$, $i = 1, ..., n$, such that for each transmission path, the sum of the downlink network interface delay, $\check{T}_{dl,i}(t)$, $i = 1, ..., n$, and the queue dwell time $\check{T}_{queue,i}(t)$, $i = 1, ..., n$, is regulated to the same value by the corresponding inner control loop. When this is successful, the delay skews from the splitter node to the air interfaces between all transmission paths are zero. As shown in section II-A, biases can be added to obtain regulation to arbitrary delay skews. The input signals to the delay skew controller are the queue reference values $\check{T}^{ref}_{queue,i}(t)$, $i = 1, ..., n$, for each transmission path, and the output signals are the queue dwell times, $\check{T}_{queue,i}(t)$, $i = 1, ..., n$, of each transmission queue.

A. Outer queue dwell time reference signal compensation

To derive the outer queue dwell time adjustment mechanism, $\mathbf{M}$, it is assumed that e.g. time stamping is applied to measure the downlink network interface delays $\check{T}_{dl,i}(t)$, $i = 1, ..., n$. This requires that the following condition holds

C1) The splitter node and the transmission nodes are either synchronized, or the relative differences between their clocks are known.

The average downlink network interface delay is given by

$$\check{\bar{T}}_{dl}(t) = \frac{1}{n}\sum_{k=1}^{n}\check{T}_{dl,k}(t). \tag{1}$$

This gives the following transmission path deviations from $\check{\bar{T}}_{dl}(t)$

$$\Delta\check{T}_{skew,i}(t) = \check{T}_{dl,i}(t) - \check{\bar{T}}_{dl}(t)$$
$$= \frac{n-1}{n}\check{T}_{dl,i}(t) - \frac{1}{n}\sum_{i\neq k=1}^{n}\check{T}_{dl,k}(t), \quad i = 1, ..., n. \tag{2}$$

By compensating $\check{T}^{ref}_{queue,i}(t)$, $i = 1, ..., n$, with the negative of $\Delta\check{T}_{skew,i}(t)$, $i = 1, ..., n$, the consequence is that the queue dwell time reference values are adjusted to set the desired total delays for data packets traveling from the splitter node to the wireless interfaces to achieve desired values, irrespective of the delay of the transmission path. In case of equal $\check{T}^{ref}_{queue,i}(t)$, $i = 1, ..., n$, the related values are the same, resulting in zero delay skew at the wireless interfaces. To see this, note that when the reference values are approximately met by the control loops, (1) and (2) show that the total travel times become

$$\check{T}_i(t) = \check{T}_{dl,i}(t) + \check{T}_{queue,i}(t)$$

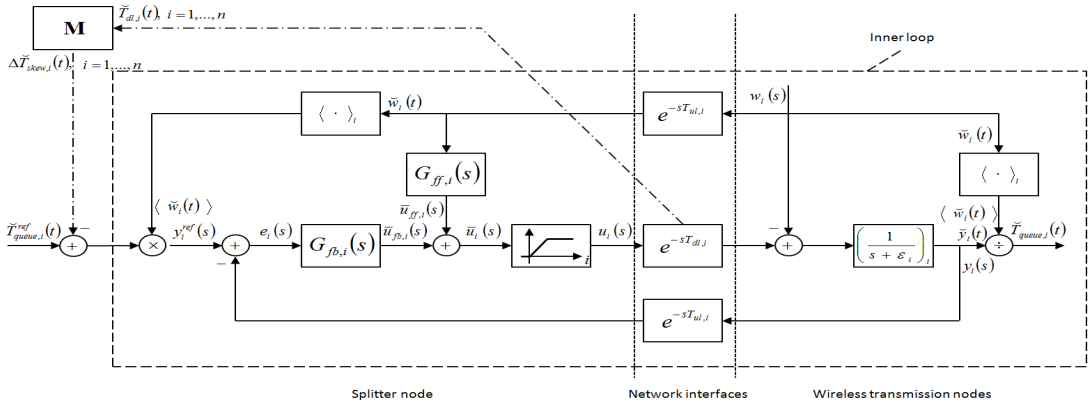

Fig. 2. Block diagram of the proposed delay skew controller.

$$\approx \check{T}_{dl,i}(t) + \check{T}^{ref}_{queue,i}(t) - \Delta\check{T}_{skew,i}(t)$$

$$= \check{T}^{ref}_{queue,i}(t) + \frac{1}{n}\sum_{k}^{n}\check{T}_{dl,k}(t)$$

$$= \check{T}^{ref}_{queue,i}(t) + \breve{\bar{T}}_{dl}(t), \quad i = 1, ..., n. \tag{3}$$

Equation (3) corresponds to using a delay skew reference value between transmission paths i and j, $\check{T}^{ref}_{skew,i,j}(t)$, that is given by

$$\check{T}^{ref}_{skew,i,j}(t) = \check{T}^{ref}_{queue,i}(t) + \breve{\bar{T}}_{dl}(t) - \check{T}^{ref}_{queue,j}(t) - \breve{\bar{T}}_{dl}(t)$$
$$= \check{T}^{ref}_{queue,i}(t) - \check{T}^{ref}_{queue,j}(t), \ i = 1, ..., n, \ j = 1, ...n. \tag{4}$$

Note again that in case $\check{T}^{ref}_{queue,i}(t)$, $i = 1, ..., n$, are chosen equal, the delay skews will be regulated towards zero.

Then define the vectors

$$\check{\mathbf{T}}^{ref}_{queue}(t) = \left(\check{T}^{ref}_{queue,1}(t) \ ... \ \check{T}^{ref}_{queue,n}(t)\right)^T, \tag{5}$$

$$\Delta\check{\mathbf{T}}_{skew}(t) = \left(\Delta\check{T}_{skew,1}(t) \ ... \ \Delta\check{T}_{skew,n}(t)\right)^T, \tag{6}$$

$$\check{\mathbf{T}}_{dl}(t) = \left(\check{T}_{dl,1}(t) \ ... \ \check{T}_{dl,n}(t)\right)^T. \tag{7}$$

By writing (2) in matrix form to describe the static matrix $\mathbf{M}$ of Fig. 2 the following result is obtained

Theorem 1: Assume that C1 holds and that $\check{\mathbf{T}}^{ref}_{queue}(t)$ is additively compensated with $-\Delta\check{\mathbf{T}}_{skew}(t)$, where $\Delta\check{\mathbf{T}}_{skew}(t) = \mathbf{M}\check{\mathbf{T}}_{dl}(t)$ and where $\mathbf{M}$ of Fig. 2 is given by

$$\mathbf{M} = \frac{1}{n}\begin{pmatrix} n-1 & -1 & \cdots & -1 \\ -1 & n-1 & -1 & \vdots \\ \vdots & & & -1 \\ -1 & \cdots & -1 & n-1 \end{pmatrix}.$$

Then this corresponds to using downlink delay skew reference values given by $\check{T}^{ref}_{skew,i,j}(t) = \check{T}^{ref}_{queue,i}(t) - \check{T}^{ref}_{queue,j}(t)$, $i = 1, ..., n$, $j = 1, ..., n$.

Remark 1: Matrix $\mathbf{M}$ equals the upper left block of the static decoupling matrix of [9], with the normalization factor changed from $n+1$ to n. The same mechanism as in the present paper is needed also in [9], albeit in another setting.

B. Inner loops

The n inner control loops depicted within dashed lines in Fig. 2 have the same structure as the flow control loop discussed in [18]. The same inner loop control structure is used in [9], [19] and [20] as well, and therefore the description of the present paper is limited to an overview. The control loop with index i is used in the following description.

1) Embedding: The inner loop applies embedding [18], which transforms the time varying queue dwell time control problem into a time invariant queue data volume control problem. The advantage is that the many *time invariant* controller design methods of the literature can be applied. In addition, the transformation to a time-invariant control loop allows the application of the Popov criterion later in the paper. The time invariant embedding consists of multiplication of the compensated queue dwell reference by the averaged wireless data rate, $\langle\breve{w}_i(t)\rangle_i$, $i = 1, ..., n$, to produce the reference value $y_i^{ref}(s)$, $i = 1, ..., n$, for the queue data volume controllers. Here the description therefore can switch to the Laplace transform domain, s. At the output of the inner control loop the queue data volume $y_i(s)$, $i = 1, ..., n$, is transformed to the time domain, t, to terminate the embedding by a division of $\breve{y}_i(t)$, $i = 1, ..., n$, by $\langle\breve{w}_i(t)\rangle_i$, $i = 1, ..., n$. This transforms back to the corresponding queue dwell time $\check{T}_{queue,i}(t)$, $i = 1, ..., n$. The inner loop is therefore closed from the queue data volume and not from the queue dwell time. The reader is referred to e.g. [19] for further details on the embedding.

2) Time invariant inner loop feedforward control: The time invariant inner loop utilizes a combination of feedforward and feedback control. The feedforward controller uses delayed measurements of the wireless data rate, $e^{-sT_{ul,i}}w_i(s)$, $i = 1, ..., n$, to cancel as much as possible of the direct effect of $w_i(s)$, $i = 1, ..., n$, on the data volume state of the queue. By neglecting the saturation and referring to Fig. 2, this can be achieved by selection of a feedforward controller $G_{ff,i}(s)$, $i = 1, ..., n$, that is such that

$$e^{-s(T_{dl,i}+T_{ul,i})}G_{ff,i}(s) \approx 1, \ i = 1, ..., n. \tag{8}$$

However, such a controller is infeasible. In the present paper a feedforward controller filter given by

$$G_{ff,i}(s) = \frac{T_{ff,1,i}s + 1}{T_{ff,2,i}^2 s^2 + 2T_{ff,2,i}s + 1},\ i = 1, ..., n \quad (9)$$

is used. Here $T_{ff,1,i}$, $i = 1, ..., n$, and $T_{ff,2,i}$, $i = 1, ..., n$, are filter parameters. The feedforward filter provides a *prediction* ahead in time of $T_{ff,1,i}$, $i = 1, ..., n$, seconds, together with low pass filtering to suppress noise, c.f. [18]. The tuning of the filter is further discussed in section IV-A.

3) Time invariant inner loop feedback control: Since the delays of the loop prevent an exact cancelation of $w_i(s)$, $i = 1, ..., n$, the feedback part of the inner loop controller regulates away low frequency components of the remaining control error. A leaky proportional-integral (PI) controller [25] is used for that purpose and is given by

$$G_{fb,i}(s) = K_{P,i} + \frac{K_{I,i}}{s + \alpha_i},\ i = 1, ..., n. \quad (10)$$

The controller parameters are hence given by $K_{P,i}$, $i = 1, ..., n$, $K_{I,i}$, $i = 1, ..., n$ and α_i, $i = 1, ..., n$,. The reason behind the leakage is again the conditions for the stability analysis that applies the Popov-criterion [26]. The tuning of $G_{fb,i}(s)$, $i = 1, ..., n$, is further discussed in section IV-A.

4) Leaky AQM queue dynamics: In practice, an AQM algorithm operating in an end-to-end overlaid fashion is often used in parallel to the controller of the present paper. As a model of AQM, data discarding proportional to the data volume of the transmit data queue is assumed here, with the proportionality factor being denoted ε_i, $i = 1, ..., n$. This choice of model is reasonable since a high data volume needs more data discards. With AQM added, Fig. 2 then results in the following differential equations for the data volume in the transmit data queues

$$\frac{d\breve{y}_i(t)}{dt} = \breve{u}_i(t - T_{dl,i}) - \breve{w}_i(t) - \varepsilon_i \breve{y}_i(t),\ i = 1, ..., n. \quad (11)$$

5) Time invariant control loop: The time invariant inner control loop can now be described. First the control error, $e_i(s)$, $i = 1, ..., n$, is computed in the splitter node, using the delayed feedback measurement, $e^{-sT_{ul,i}}y_i(s)$, $i = 1, ..., n$. received from the wireless transmission node, to obtain

$$e_i(s) = y_i^{ref}(s) - e^{-sT_{ul,i}}y_i(s),\ i = 1, ..., n. \quad (12)$$

The feedback control signal component follows as

$$\bar{u}_{fb,i}(s) = G_{fb,i}(s)e_i(s),\ i = 1, ..., n. \quad (13)$$

The feedforward control signal component given by

$$\bar{u}_{ff,i}(s) = G_{ff,i}(s)e^{-sT_{ul,i}}w_i(s),\ i = 1, ..., n, \quad (14)$$

is then added to $u_{fb,i}(s)$, $i = 1, ..., n$, to give

$$\bar{u}_i(s) = \bar{u}_{fb,i}(s) + \bar{u}_{ff,i}(s),\ i = 1, ..., n. \quad (15)$$

The control signal $\bar{u}_i(s)$, $i = 1, ..., n$, represents the commanded downlink data rate, at which packets are sent to the wireless transmission queue of transmission node i. Since the data flow is one-directional, the commanded data rate must be nonnegative. It is also limited to below the capacity of the network interface as motivated by Shannon's data rate theorem [6]. The inner loop controller secures these properties by application of a static nonlinear saturation. This saturation operates in the time domain, and it is given by

$$\breve{u}_i(t) = \begin{cases} \bar{u}_{max,i}, & \breve{\bar{u}}_i(t) \geq \bar{u}_{max,i} \\ \breve{\bar{u}}_i(t), & \bar{u}_{min,i} < \breve{\bar{u}}_i(t) < \bar{u}_{max,i} \\ \bar{u}_{min,i}, & \breve{\bar{u}}_i(t) \leq \bar{u}_{min,i} \end{cases} \quad (16)$$

The control signal data rate $\breve{u}_i(t)$, $i = 1, ..., n$, is then applied for packet data transmission over the network interface i, leading to the following equation for the data volume dynamics of the wireless transmission node

$$y_i(s) = \frac{1}{s + \varepsilon_i}\left(e^{-sT_{dl,i}}u_i(s) - w_i(s)\right). \quad (17)$$

This completes the description of the delay skew controller.

III. Input-output stability

To prove $\mathcal{L}_2$-stability for the MIMO control system of Fig. 2, the key observation is that there is no state feedback involved in the reference computation mechanism. This observation reduces the stability analysis to a stability analysis of each separate inner loop of the MIMO controller.

To proceed, it is noted that the leaky PI-controllers used as feedback filters in the present paper constitute lag-parts of the lead-lag controller of [18]. Furthermore, the feedforward filters are the same as those in [18]. It is therefore suitable to build on the input-output stability analysis of that paper when analyzing the input-output stability of the control system of the present paper. The main result of [18] that is applied here proves $\mathcal{L}_2$-stability for an inner control loop similar to the one of the present paper. The only difference is that the feedback controller of [18] is the more general case of a lead-lag controller of the following form:

$$G_{leadlag,i}(s) = K_i\frac{s + a_i}{s + \frac{a_i}{M_i}}N_i\frac{s + b_i}{s + b_iN_i},\ i = 1, ..., n, \quad (18)$$

where K_i, a_i, M_i, b_i, N_i, $i = 1, ..., n$, are controller parameters, explained in detail in [18]. A repeated application of Theorem 1 of [18] can therefore be used to prove $\mathcal{L}_2$-stability of the delay skew controller of the present paper.

Theorem 1 of [18] is based on the conditions numbered A1-A9 listed in that paper. To state the desired result, the following conditions that result when the conditions A1-A9 of [18] are applied to the inner loops of the present paper, are therefore required to hold:

- C2) The difference $|\breve{u}_{c,i}(t) - \breve{u}_{d,i}(t)| \to 0$ when the sampling period $T_s \to 0$, where $\breve{u}_{c,i}(t)$ and $\breve{u}_{d,i}(t)$ denote the continuous time and discrete time control signals, $i = 1, ..., n$.
- C3) The controlled packet queue is linear.
- C4) The delays $T_{ul,i}$ and $T_{dl,i}$, $i = 1, ..., n$, are constant.
- C5) $0 < w_{min} \leq \breve{w}_i(t) \leq w_{max} < \infty, \forall t,\ i = 1, ..., n$.
- C6) $\varepsilon_i > 0$.
- C7) $a_i > 0$, $b_i > 0$, $N_i > 0$, $K_i > 0$ and $0 < M_i < M_{max} < \infty$, $i = 1, ..., n$.

C8) $\check{w}_i \in \mathcal{L}_2$ and $\check{\dot{w}}_i \in \mathcal{L}_2$, $i = 1, ..., n$.
C9) $\check{T}^{ref}_{queue,i}(t) - \Delta\check{T}_{skew,i}(t)$, $i = 1, .., n$ is constant.
C10) $T_{ff,1,i} > 0$ and $T_{ff,2,i} > 0$ for $i = 1, ..., n$.

The condition C2 is typically met, provided that the sampling scheme is well-behaved as when the Tustin-approximation is used, c.f. [24]. The conditions C3, C4, C6, C7 and C10 are easily enforced when tuning the inner-loop controllers. C5 is always fulfilled in practice, while C8 is a direct consequence of the conditions that underpin the Popov-criterion. The condition C8 ensures that the frequency contents of $\check{w}_i$ rolls off sufficiently fast to prevent any high frequency parts from triggering instability. The condition C4 limits the scope of the result, a relaxation would however require IQC analysis [22] which is beyond the scope of this paper. One advantage is that C4 implies that $\Delta\check{T}_{skew,i}(t)$, $i = 1, .., n$, is constant. Fig. 2 then leads to the conclusion that C9 needs to hold for A8 of [18] to be implied. In summary, the conditions A1-A9 of [18] are therefore implied by conditions C2-C10 above.

Finally note that since

$$G_{fb,i}(s) = K_{p,i} + \frac{K_{I,i}}{s + \alpha_i} = K_{P,i}\frac{s + \alpha_i + K_{I,i}/K_{P,i}}{s + \alpha_i}, \tag{19}$$

with $i = 1, ..., n$, a selection of $N_i = 1$ reduces the lead link of the controller of [18] to 1, which shows that $G_{fb,i}(s)$, $i = 1, .., n$, are special cases of the lead-lag controller treated in [18]. This proves:

Theorem 2: Consider the delay skew control system of Fig. 2 with $G_{ff,i}(s) = K_{P,i} + K_{I,i}/(s + \alpha_i)$, $i = 1, ..., n$, and leaky queue dynamics given by $1/(s + \varepsilon_i)$, $i = 1, ..., n$. Assume that C1-C10 hold. Then the delay skew control system is $\mathcal{L}_2$-stable if there exist constants q_i, $\delta_i > 0$, $i = 1, ..., n$, such that the Popov plots of

$$\hat{g}_i(s) = \frac{e^{-s(T_{ul,i}+T_{dl,i})}}{s + \varepsilon_i} K_{P,i}\frac{s + \alpha_i + K_{I,i}/K_{P,i}}{s + \alpha_i},$$

given by

$$\omega \in [0, \infty) \rightarrow Re[\hat{g}_i(j\omega)] + j\omega Im[\hat{g}_i(j\omega)] \in C, i = 1, ..., n.$$

lie entirely to the right of lines through $-1 + \delta_i + j0$ with slope $1/q_i$, for some $q_i \geq 0$ and some $\delta_i > 0$, $i = 1, ..., n$.

Remark 2: Theorem 1 provides an easy to use graphical stability test, c.f. [26]. The geometrical condition on the Popov plots are equivalent to the following inequalities. For $i = 1, \ldots, n$ there exists $q_i > 0$ such that

$$Re[(1 + j\omega q_i)\hat{g}_i(j\omega)] + 1 \geq \delta_i > 0, \ \forall \omega \geq 0. \tag{20}$$

These inequalities, one for each transmission path, allow the subsets of the stability regions defined by (20) to be pre-computed in terms of e.g. the maximum allowable network interface delays, c.f. [18], [27]–[29]. This leads to the conclusion that the proposed delay skew controller is globally $\mathcal{L}_2$-stable up to a set of maximum pre-computable network interface delays.

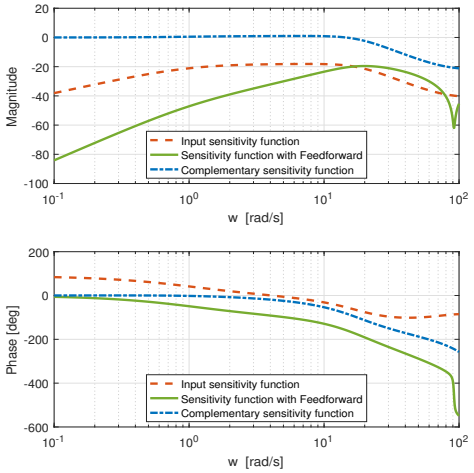

Fig. 3. Second inner control loop: sensitivity function (red-dashed line), sensitivity function with the effect of feedforward included (green-continuous line), and the complementary sensitivity function (blue dot-dashed line).

IV. Numerical results

PI control is a well-known technology with numerous applications [25]. This fact alone is a strong motivation to apply it also for delay skew control. This is one reason why the numerical evaluation is performed for the limiting case where $\varepsilon_i = 0$, $i = 1, ..., n$ and $\alpha_i = 0$, $i = 1, ..., n$.

A. Scenario and controller tuning

In the numerical scenario of the paper, the network interface delays of the two transmission paths were $T_{dl,1} = T_{ul,1} = 0.005$ s and $T_{dl,2} = T_{ul,2} = 0.03$ s, respectively. The reference values for the dwell times of the transmission node queues were set to $T^{ref}_{queue,1} = T^{ref}_{queue,2} = 0.065$ s.

The parameters of the feedforward controller filters of (9) were selected as $T_{ff,2,i} = 0.02$ s, $i = 1, 2$, after which the prediction parameters were selected as $T_{ff,1,i} = (T_{dl,2} + T_{ul,2} + 2T_{ff,2,i})/2 = 0.05$ s, $i = 1, 2$. This was done to achieve a prediction time close to the worst case round trip delay and to have a settling time of the feedforward controller that was faster than the prediction time interval. This choice was tested in simulations and allows for prediction of disturbances for substantial fractions of the reference queue dwell time values.

The feedback controller parameters of (10) were tuned to regulate away remaining low frequency errors. The parameters used were $K_{P,i} = 9$, $i = 1, 2$, and $K_{I,i} = 8$, $i = 1, 2$.

It can be shown that the input sensitivity function, defined as the transfer function from the disturbance $w_i(s)$, $i = 1, 2$, to the output $y_i(s)$, $i = 1, 2$, and neglecting the nonlinearity and feedforward contribution is given by

$$S_i(s) = \frac{s}{s^2 + (K_{P,i}s + K_{I,i})e^{-s(T_{dl,i}+T_{ul,i})}}, \ i = 1, ..., 2. \tag{21}$$

It is plotted with a red-dashed line in Fig. 3, for the second transmission path and it is evident that it behaves as stated above. To illustrate the effect of the feedforward controller,

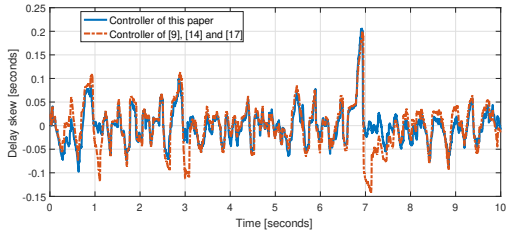

Fig. 4. The time evolution over 10 s of the delay skew measured in seconds when controlled by the controller of the present paper (blue-continuous line) and when controlled by the controller of [9], [19] and [20] (red dot-dashed line).

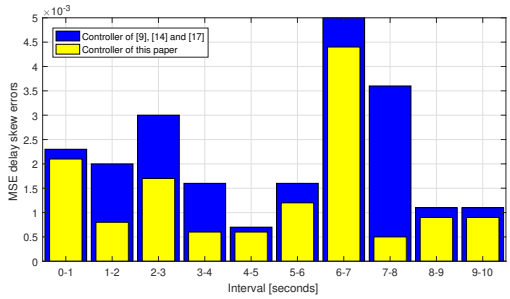

Fig. 5. Comparison of the MSE Delay Skew Errors for the proposed controller and the controller of [9], [19] and [20].

the sensitivity function accounting also for $G_{ff,i}(s)$, $i = 1, 2$, of (9) for $i = 2$ is plotted with a green-continuous in Fig. 3. That sensitivity function is given by

$$\bar{S}_i(s) = \left(G_{ff,i}(s)e^{-s(T_{dl,i}+T_{ul,i})} - 1\right) S_i(s), \;\; i = 1, 2, \tag{22}$$

which is verified from Fig. 2. Notice that the feedforward controller reduces the sensitivity significantly. Finally, the complementary sensitivity function is depicted with a blue dot-dashed line in Fig. 3. The saturation is again neglected.

B. Simulation results

In this section the delay skew controller of the present paper is compared to the one described in [9], [19] and [20]. The traffic data represented a full buffer case. The wireless rates were generated with a system simulator, including radio modeling, link adaptation and scheduling functionality.

Snapshots of the simulation results are depicted in Fig. 4 and Fig. 6. Fig. 4 shows the time evolution of the delay skew measured at the wireless interfaces. When comparing, the controller of the present paper appears to be more stable, with a smaller variation of the delay skew than the controller of [9], [19] and [20] that includes an outer delay skew feedback control loop. This slight advantage for the delay skew controller proposed in the present paper is supported by the measurements of mean squared delay skew errors per second, that appear in Fig. 5. To provide a more detailed comparison of the performance of the controller of the present paper and the one of [9], [19] and [20], the simulated queue data volumes are addressed by Fig. 6. These plots indicate that the data volume reference value variations are

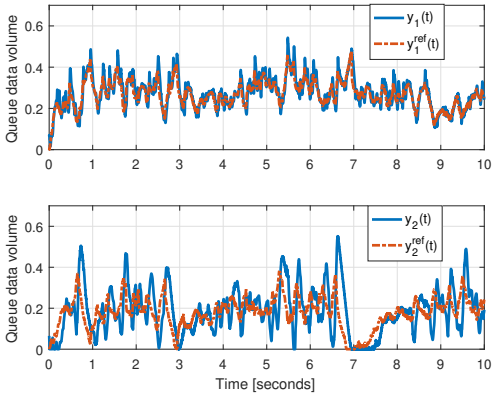

(a) The controller of [9], [19] and [20].

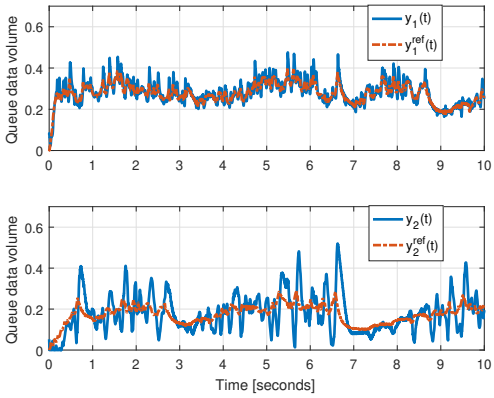

(b) The controller of the present paper.

Fig. 6. The time evolution over 10 s of the normalized queue data volumes and queue data volume references measured in Mbits when controlled by (a) the controller of [9], [19] and [20]; (b) the proposed controller.

the reason for the difference between the alternatives, since the inner loop controllers of the present paper and the ones of [9], [19] and [20] are identically tuned. This suggests that the difference can be explained by an analysis of the effect of the outer loop of [9], [19] and [20], as compared to the use of the reference value adjustment mechanism of the present paper.

V. Discussion

Contrary to the delay skew controller described in [9], [19] and [20], the controller of the present paper does not have an outer delay skew control loop. This may explain the somewhat better performance of the controller of the present paper, since under normal operation an additional outer loop might lead to a phase margin that is worse than when using the static adjustment mechanism of the present paper. Such an effect would increase the variation of the delay skews of the controller of [9], [19] and [20]. However, in case the dynamics of the transmission paths of the delay skew control system would be more complicated than single queues and single delays, the situation may be different. In such situations the delay skew controller of [9], [19] and [20] has the advantage of measured delay skew feedback signals. The outer loop can then compensate for the un-

modeled dynamics with its relatively high low frequency gain. This would adjust the reference delays for the inner loops to values that would regulate the delay skews towards zero, despite the un-modeled dynamics. There is hence a tradeoff between the robustness of the controller of [9], [19] and [20], and the simplicity and better stability of the delay skew controller of the present paper.

VI. Conclusion

The paper presented a new networked controller for downlink delay skew control in 5G wireless networks with multi-point transmission. Potential use cases include e.g. augmented reality application using overlaid real time video, and situations where media applications require video and audio data to be sent to different devices, and where synchronization needs to be maintained to avoid a reduced end user experience. The main theoretical contribution of the paper consists of a proof of the global input-output $\mathcal{L}_2$-stability of the proposed delay skew control system. The performance of the proposed controller was evaluated with simulations. The advantages and disadvantages with respect to delay skew control architectures that exploit delay skew feedback signals were discussed as well.

There are several opportunities to do additional research in the delay skew control field. The stability analysis could be extended to consider also time varying delays. This is an important engineering topic, since stability is a guarantee for uniform and consistent performance. Since the delay skew control problem includes positivity constraints on the data rates over the network interfaces, it would also be interesting to study model predictive control to account for this, see [30], [31].

VII. Acknowledgements

This research was supported under Australian Research Council's Linkage Projects funding scheme (project number LP150100757).

References

[1] S. A. Ashraf, I. Aktas, E. Eriksson, K. W. Helmersson, and J. Ansari, "Ultra-reliable and low-latency communication for wireless factory automation: From LTE to 5G," in *2016 IEEE 21st International Conference on Emerging Technologies and Factory Automation (ETFA)*. IEEE, Sep. 2016.

[2] K. Pretz, "The future of communications networks," *the institute*, vol. 41, no. 1, pp. 6–7, 2017.

[3] T. Marugame, A. Kamikura, M. Ohnishi, and M. Nakagawa, "Evaluation on effect of errors on haptic information in wireless communication system," in *Proc. 2003 IEEE/RSJ International Conference on Intelligent Robots and Systems (IROS)*, 2003.

[4] K. Pretz, "Gerhard Fettweis: Developing 5G and beyond," *the institute*, vol. 41, no. 1, p. 14, 2017.

[5] T. Samad, "Control systems and the internet of things," *IEEE Control Systems*, vol. 36, no. 1, pp. 13–16, 2016.

[6] T. S. Rappaport, R. W. Heath Jr., R. C. Daniels, and J. N. Murdock, *Millimeter Wave Wireless Communications*. Westford, Massachusetts: Prentice Hall, 2014.

[7] T. Bonald, M. May, and J.-C. Bolot, "Analytic evaluation of RED performance," in *Proc. IEEE INFOCOM 2000. Conference on Computer Communications. 19th Annual Joint Conference of the IEEE Computer and Communications Societies*, 2000.

[8] R. Srikant and L. Ying, *Communication Networks - An Optimization, Control and Stochastic Networks Perspective*. Padstow Cornwall, UK: Cambridge University Press, 2014.

[9] K. Lau, T. Wigren, R. Delgado, and R. H. Middleton, "Disturbance rejection properties for a 5G networked data flow delay controller," in *2017 IEEE 56th Annual Conference on Decision and Control (CDC)*. IEEE, Dec. 2017.

[10] R. Luck and A. Ray, "An observer-based compensator for distributed delays," *Automatica*, vol. 26, no. 5, pp. 903–908, Sep. 1990.

[11] A. Cuenca, P. García, P. Albertos, and J. Salt, "A non-uniform predictor-observer for a networked control system," *International Journal of Control, Automation and Systems*, vol. 9, no. 6, pp. 1194–1202, Dec 2011.

[12] R. Imai and R. Kubo, "Introducing jitter buffers in networked control systems with communication disturbance observer under time-varying communication delays," in *IECON 2015 - 41st Conference of the IEEE Industrial Electronics Society*. IEEE, nov 2015, pp. 2956–2961.

[13] C. Sreenan, J.-C. Chen, P. Agrawal, and B. Narendran, "Delay reduction techniques for playout buffering," *IEEE Transactions on Multimedia*, vol. 2, no. 2, pp. 88–100, Jun. 2000.

[14] R. H. Middleton, T. Wigren, K. Lau, and R. A. Delgado, "Data flow delay equalization for feedback control applications using 5G wireless dual connectivity," in *2017 IEEE 85th Vehicular Technology Conference (VTC Spring)*, Jun. 2017.

[15] V. M. Popov, "Nouveaux criteriums de stabilité pour les systemés automatiques non-linèaries," *Revue d´Electrotechnique et d´Energetique, Acad. de la Rep. Populaire Romaine*, vol. 5, no. 1, 1960.

[16] G. Zames, "Functional analysis applied to nonlinear feedback systems," *IEEE Transactions on Circuit Theory*, vol. 10, no. 3, pp. 392–404, Sep. 1963.

[17] ——, "On the input-output stability of time-varying nonlinear feedback systems part one: Conditions derived using concepts of loop gain, conicity, and positivity," *IEEE Transactions on Automatic Control*, vol. 11, no. 2, pp. 228–238, Apr. 1966.

[18] T. Wigren, "Robust $\mathcal{L}_2$ stable networked control of wireless packet queues in delayed internet connections," *IEEE Transactions on Control Systems Technology*, vol. 24, no. 2, pp. 502–513, 2015.

[19] T. Wigren, K. Lau, R. A. Delgado, and R. H. Middleton, "Delay skew packet flow control in wireless systems with dual connectivity," *IEEE Transactions on Vehicular Technology*, vol. 67, no. 6, pp. 5357–5371, Jun. 2018.

[20] R. A. Delgado, T. Wigren, K. Lau, and R. H. Middleton, "Stability properties of a MIMO data flow controller," in *2018 American Control Conference (ACC)*, Milwaukee, USA, Jun. 2018, pp. 2638–2643.

[21] R. A. Delgado, K. Lau, R. H. Middleton, and T. Wigren, "Networked delay control for 5G wireless machine type communications using multi-connectivity," *to appear in IEEE Transactions on Control Systems Technology*, 2018.

[22] C. Y. Kao and A. Rantzer, "Stability analysis of systems with uncertain time-varying delays," *Automatica*, vol. 43, no. 6, pp. 959–979, 2007.

[23] T. Wigren, K. Lau, R. A. Delgado, and R. H. Middleton, "Globally stable delay alignment for feedback control over NR multi-point connections," *submitted to IEEE Trans. Contr. Network Systems*, 2018.

[24] A. V. Oppenheim and R. W. Schafer, *Digital Signal Processing*. Englewoof Cliffs, NJ: Prentice Hall, 1975.

[25] K. J. Åström and T. Hägglund, *Advanced PID control*. ISA-The Instrumentation, Systems, and Automation Society, 2006.

[26] M. Vidyasagar, *Nonlinear Systems Analysis*. Englewood Cliffs, NJ: Prentice-Hall, 1978.

[27] T. Wigren, "Wireless feedback and feedforward data flow control subject to rate saturation and uncertain delay," *IET Control Theory & Applications*, vol. 10, no. 3, pp. 346–353, Feb. 2016.

[28] ——, "Low frequency sensitivity function constraints for nonlinear $\mathcal{L}_2$-stable networked control," *Asian Journal of Control*, vol. 18, no. 4, pp. 1200–1218, 2016.

[29] ——, "Loop-shaping feedback and feedforward control for networked systems with saturation and delay," *Asian Journal of Control*, vol. 19, no. 4, pp. 1329–1349, Dec. 2016.

[30] G. C. Goodwin, A. M. Medioli, D. S. Carrasco, B. R. King, and Y. Fu, "A fundamental control limitation for linear positive systems with application to type 1 diabetes treatment," *Automatica*, vol. 55, pp. 73–77, May 2015.

[31] G. C. Goodwin, M. M. Seron, and J. A. DeDona, *Constrained Control and Estimation - An Optimization Approach*. London, UK: Springer-Verlag, 2005.